

NACA TN 3461 7746

TECH LIBRARY KAFB, NM  
006579

# NATIONAL ADVISORY COMMITTEE FOR AERONAUTICS

TECHNICAL NOTE 3461

TURBULENT-HEAT-TRANSFER MEASUREMENTS AT

A MACH NUMBER OF 1.62

By Maurice J. Brevoort and Bernard Rashis

Langley Aeronautical Laboratory  
Langley Field, Va.



Washington  
June 1955

NACA  
TECHNICAL LIBRARY  
AFL 2811



0066579

## NATIONAL ADVISORY COMMITTEE FOR AERONAUTICS

## TECHNICAL NOTE 3461

## TURBULENT-HEAT-TRANSFER MEASUREMENTS AT

A MACH NUMBER OF 1.62

By Maurice J. Brevoort and Bernard Rashis

## SUMMARY

Turbulent-heat-transfer measurements were obtained through the use of an axially symmetric annular nozzle which consists of an inner, shaped center body and an outer cylindrical sleeve. Measurements taken along the outer sleeve gave essentially flat-plate results that are free from wall interference and corner effects for a Mach number of 1.62 and for a Reynolds number range of  $7.22 \times 10^5$  to  $1.20 \times 10^8$ . The heat-transfer coefficients are in good agreement with theoretical results for a Mach number of 1.60 and for a ratio of inner-surface to free-stream temperature of 1.60. The temperature-recovery factors are on the average 1.5 percent lower than the factors obtained for a Mach number of 2.4.

## INTRODUCTION

The design of supersonic aircraft and missiles requires engineering information about heat-transfer coefficients and temperature-recovery factors for supersonic speeds that extend over a wide range of Reynolds number. In references 1 and 2, local turbulent-heat-transfer measurements were presented for Mach numbers of 3.03 and 2.06, respectively.

The purpose of this investigation is to extend the work of references 1 and 2, with the same type of apparatus and method of reducing the data, to a Mach number of 1.62. The range of Reynolds number for which measurements were obtained is from  $7.22 \times 10^5$  to  $1.20 \times 10^8$ . The results cover a temperature difference of approximately  $10^\circ$  at 40 seconds after starting to approximately  $1^\circ$  at 200 seconds after starting. The average value of the ratio of inner-surface temperature to free-stream temperature  $T_w/T_\infty$  was 1.60.

## SYMBOLS

$c$	specific heat of sleeve material, Btu/lb-°R
$c_p$	specific heat of air at constant pressure, Btu/lb-°R
$g$	acceleration due to gravity, ft/sec <sup>2</sup>
$h$	heat-transfer coefficient, Btu/ft <sup>2</sup> -sec-°R
$k$	heat conductivity, Btu/ft-sec-°R
$M$	Mach number
$Nu$	Nusselt number, $hx/k$
$Pr$	Prandtl number, $\mu c_p g/k$
$R$	Reynolds number, $\rho Vx/\mu$
$St$	Stanton number, $Nu/R Pr \equiv h/\rho V c_p g$
$T_{av}$	average wall temperature, °R
$T_e$	effective stream air temperature at wall; some temperature which gives thermal potential which is independent of heat-transfer coefficient $h$ , °R
$T_t$	stagnation temperature, °R
$T_w$	inside-surface temperature of nozzle sleeve, °R
$T_\infty$	free-stream temperature, °R
$t$	time, sec
$V$	free-stream velocity, ft/sec
$w$	specific weight of sleeve material, lb/sq ft
$x$	longitudinal distance along sleeve, ft (unless indicated otherwise)
$\eta_r$	recovery factor, $\frac{T_e - T_\infty}{T_t - T_\infty}$

- $\mu$  dynamic viscosity coefficient, lb-sec/sq ft
- $\rho$  free-stream density of air, slugs/cu ft

#### APPARATUS AND METHOD

The apparatus consisted of an axially symmetric annular nozzle which was directly connected to the settling chamber of one of the cold-air blowdown jets of the Langley gas dynamics laboratory. The nozzle had a shaped wooden center body and two outer sleeves. One sleeve was constructed of 8-inch-diameter, extra heavy, seamless carbon-steel pipe, and the other was constructed of 1/16-inch stainless steel which was rolled into a cylinder and welded; both cylinders were surface-machined inside and outside to wall thicknesses of 0.388 inch and 0.060 inch, respectively. The coordinates of the inner body are given in table I.

A detailed drawing of the apparatus is shown in figure 1 which gives the location of the thermocouples and static-pressure orifices. Details of the thermocouples, the static-pressure-orifice installations, the temperature-recording equipment, and the precision of instrumentation are given in references 1 and 2.

The Mach number distribution is shown in figure 2. The alinement of the flow was checked at several stations by means of orifices located around the sleeve. The location of these measurements is shown in figure 2.

The test procedure is given in references 1 and 2. For this investigation test runs were made for settling-chamber pressures of 0.4, 57, and 196 lb/sq in. gage. The test at a pressure of 0.4 lb/sq in. gage was made with a sleeve 0.060 inch thick, and the test setup was evacuated to an absolute pressure of 1.0 inch of mercury. Excluding the first 20 seconds, the pressures were maintained constant for each test run. The stagnation temperature started at essentially room temperature and decreased as the piping was cooled, as illustrated in figure 3 where stagnation temperature is plotted against time for a settling-chamber pressure of 196 lb/sq in. gage. The wall temperature also started at essentially room temperature and tended to approach the equilibrium temperature which was approximately 22° R below stagnation temperature. This variation is shown in figure 4 where wall temperature at stations 12 and 18 is plotted against time for a settling-chamber pressure of 196 lb/sq in. gage.

In figure 5 are plotted, for various times during the test run, the values of wall temperature against longitudinal distance along the cylinder. These values were used to determine the rate of change of

the longitudinal conduction  $k \frac{d^2 T_{av}}{dx^2}$  along the cylinder. Test results were taken only for the length of the cylinder for which  $k \frac{d^2 T_{av}}{dx^2} = 0$ .

#### REDUCTION OF DATA

The method of reducing the data is completely described in references 1 and 2. Briefly, the equations used are

$$St = \frac{h}{\rho V c_p g} \quad (1)$$

$$h = wc \frac{dT_{av}/dt}{T_w - T_e} \quad (2)$$

and

$$\eta_r = \frac{T_e - T_\infty}{T_t - T_\infty} \quad (3)$$

The method consists simply of selecting a recovery factor and then obtaining  $T_e$  from equation (3). This value of  $T_e$  is substituted into equation (2) and values of  $h$  for different heat-flow ratios are obtained. These values of  $h$  are then substituted into equation (1). The true values of  $T_e$ ,  $\eta_r$ , and  $St$  are obtained when  $St$  is constant with time (for different heat-flow ratios). Figure 6 shows the values used in determining the Stanton number and recovery factor at station 12 for a settling-chamber pressure of 196 lb/sq in. gage.

The values of specific heat and specific weight of the sleeve material were taken from reference 3. The values of Prandtl number (0.71) and viscosity of air were also taken from reference 3 and were based upon  $T_w$ . The value of  $T_w$  used was the value measured 80 seconds after starting.

#### RESULTS AND DISCUSSION

Over the test range (see fig. 5), the wall temperatures are constant along  $x$ . In the relation

$$h = wc \frac{dT_{av}/dt}{T_w - T_e}$$

$w$  and  $c$  are constant, and  $dT_{av}/dt$  is constant because  $T_w$  is constant. Therefore, if there is to be a variation of  $h$  with Reynolds number or  $x$ ,  $T_e$  must vary with  $x$ . The value of  $T_e$  obtained for the test at a settling-chamber pressure of 196 lb/sq in. gage, evaluated 80 seconds after starting, actually decreases about  $1^\circ$ .

Figure 7 shows the variation of local Nusselt number with local Reynolds number. The value of  $x$  used in evaluating these numbers has been adjusted for  $x = 0$  locations (the effective beginning of the turbulent boundary layer) by the method of references 1 and 2. The  $x = 0$  locations are 4.0 and 1.0 inches downstream of the minimum station for settling-chamber pressures of 0.4 and 57 lb/sq in. gage, respectively, and at the minimum station for the settling-chamber pressure of 196 lb/sq in. gage.

The Nusselt numbers were found to vary from 840 to 56,650 for the Reynolds number range of  $7.22 \times 10^5$  to  $1.20 \times 10^8$  (based on adjusted  $x = 0$  locations.) For comparison the curve based upon the Van Driest analysis (ref. 4) is shown. For the Van Driest analysis,  $T_w/T_\infty$  was considered to be 1.60 (the average value of the test results presented herein).

The data were computed by using free-stream temperature to determine the density and velocity. The wall temperature was used to determine the viscosity and the Prandtl number. The agreement between the test results and the theory is good.

Figure 8 shows the variation of local temperature-recovery factor with local Reynolds number. The variation is from 0.880 at  $7.22 \times 10^5$  to 0.868 at  $1.20 \times 10^8$ . The results are compared with a curve which represents the fairing of the data of reference 5 for a Mach number of 2.4. The results obtained in this investigation are on the average 1.5 percent lower than the data of reference 5. Also included for comparison are the curves for the recovery factor equal to  $Pr^{1/3}$  and  $Pr^{1/2}$ . The wall temperature was used to determine the Prandtl number.

## CONCLUDING REMARKS

Turbulent-heat-transfer measurements that gave essentially flat-plate results were obtained for a Mach number of 1.62 and for a Reynolds number range of  $7.22 \times 10^5$  to  $1.20 \times 10^8$ . The Nusselt numbers agree with theoretical results. The temperature-recovery factors are on the average 1.5 percent lower than other available data for a Mach number of 2.4.

Langley Aeronautical Laboratory,  
National Advisory Committee for Aeronautics,  
Langley Field, Va., March 21, 1955.

## REFERENCES

1. Brevoort, Maurice J., and Rashis, Bernard: Turbulent-Heat-Transfer Measurements at a Mach Number of 3.03. NACA TN 3303, 1954.
2. Brevoort, Maurice J., and Rashis, Bernard: Turbulent-Heat-Transfer Measurements at a Mach Number of 2.06. NACA TN 3374, 1955.
3. Eckert, E. R. G. (With Appendix by Robert M. Drake, Jr.): Introduction to the Transfer of Heat and Mass. First ed., McGraw-Hill Book Co. Inc., 1950, pp. 266 and 274.
4. Van Driest, E. R.: The Turbulent Boundary Layer for Compressible Fluids on a Flat Plate With Heat Transfer. Rep. No. AL-997, North American Aviation, Inc., Jan. 27, 1950.
5. Stalder, Jackson R., Rubesin, Morris W., and Tendeland, Thorval: A Determination of the Laminar-, Transitional-, and Turbulent-Boundary-Layer Temperature-Recovery Factors on a Flat Plate in Supersonic Flow. NACA TN 2077, 1950.

TABLE I.- CENTER-BODY COORDINATES

x, in.	Radius, in.	x, in.	Radius, in.	x, in.	Radius, in.
-10.00	2.000	0.40	3.4249	2.10	3.2955
-4.70	2.000	.50	3.4190	2.20	3.2920
-4.50	2.020	.60	3.4122	2.30	3.2891
-4.00	2.100	.70	3.4045	2.40	3.2868
-3.00	2.500	.80	3.3961	2.50	3.2851
-2.50	2.735	.90	3.3871	2.60	3.2839
-2.00	2.970	1.00	3.3776	2.70	3.2831
-1.50	3.150	1.10	3.3680	2.80	3.2827
-1.00	3.300	1.20	3.3584	2.90	3.2825
-.80	3.340	1.30	3.3491	5.00	3.2720
-.60	3.375	1.40	3.3402	10.00	3.2470
-.40	3.400	1.50	3.3317	15.00	3.2220
-.20	3.425	1.60	3.3238	20.00	3.1970
0	3.4375	1.70	3.3167	25.00	3.1720
.10	3.4364	1.80	3.3103	30.00	3.1470
.20	3.4337	1.90	3.3047	35.00	3.1220
.30	3.4298	2.00	3.2997	38.625	3.1059

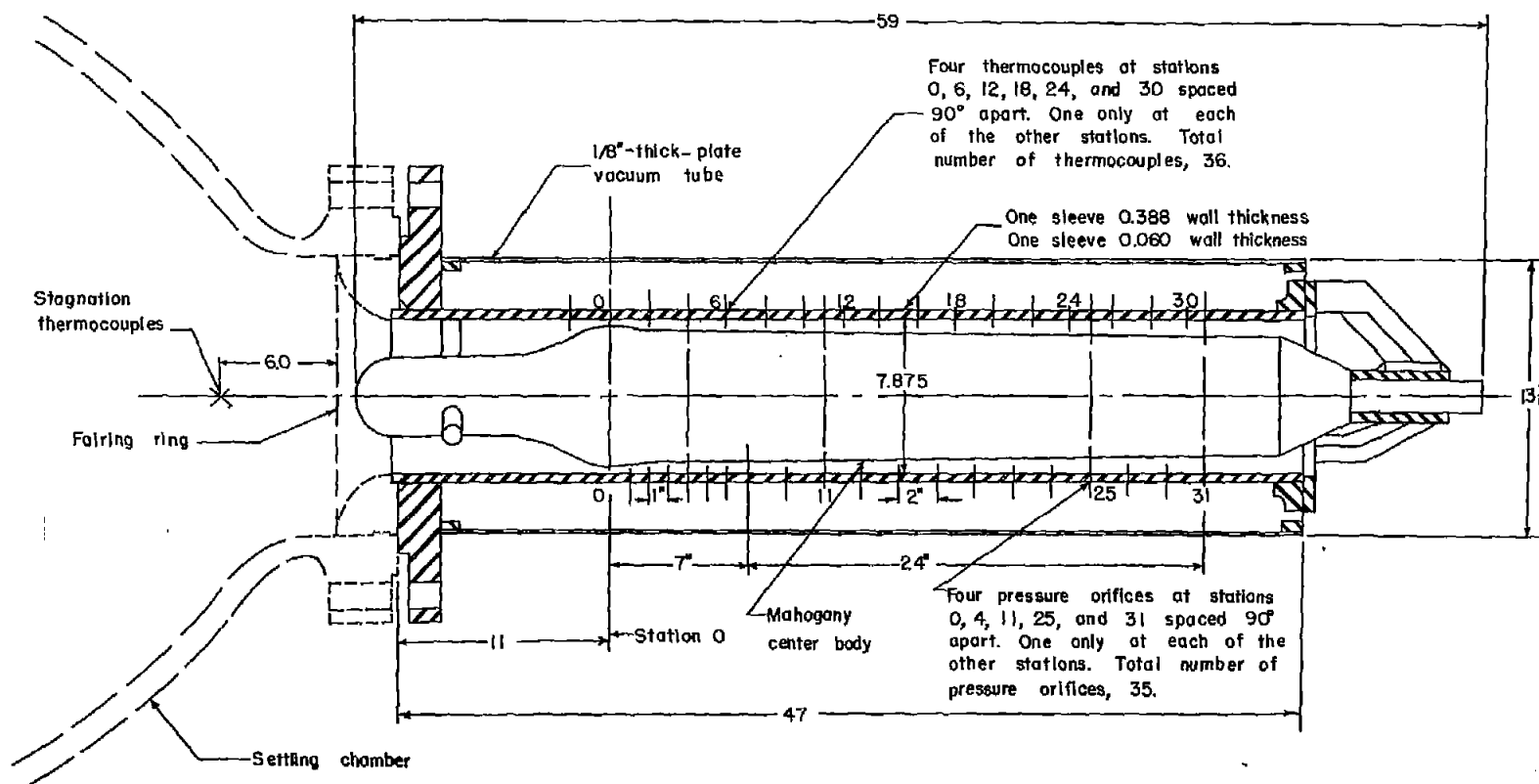


Figure 1.- Test arrangement. Dimensions are in inches.

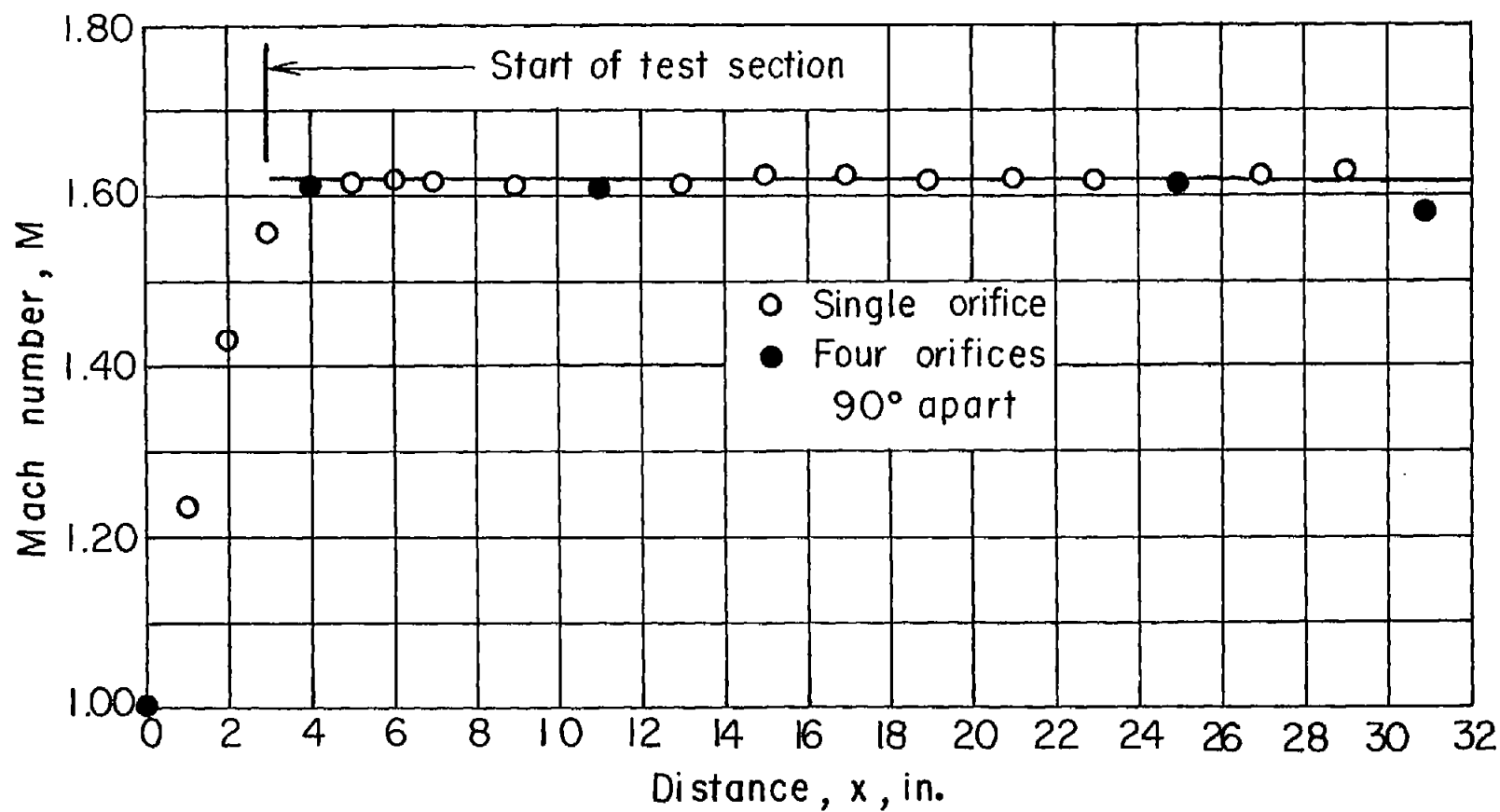


Figure 2.- Mach number distribution for settling-chamber pressure of 196 lb/sq in. gage.

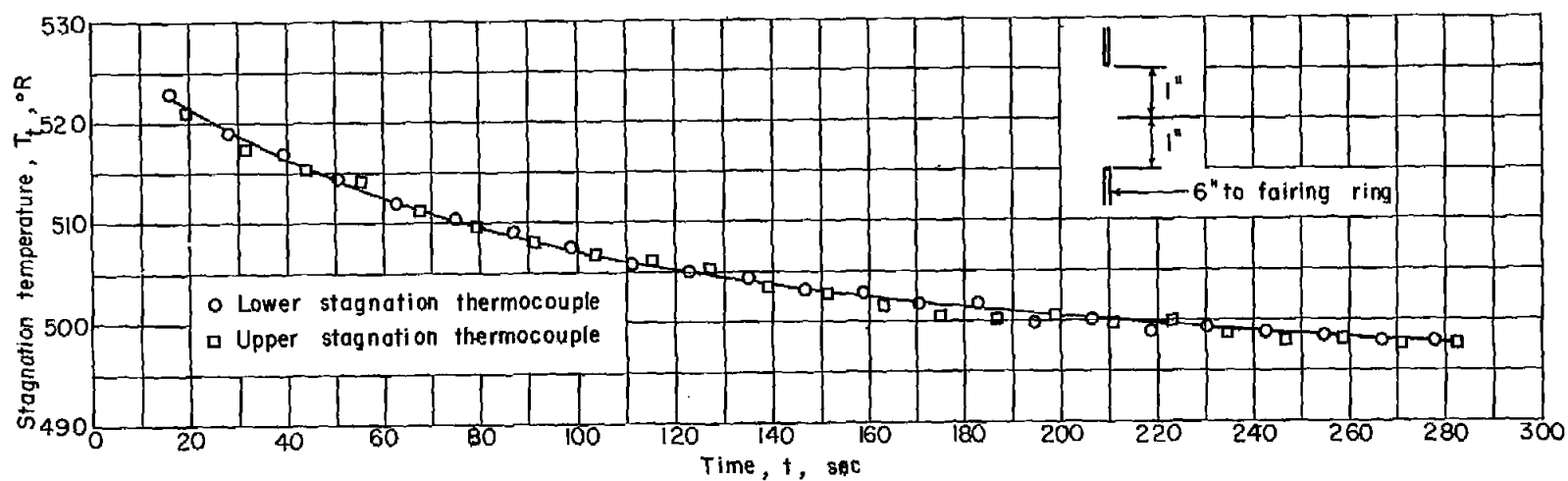


Figure 3.- Variation of stagnation temperature with time for settling-chamber pressure of 196 lb/sq in. gage.

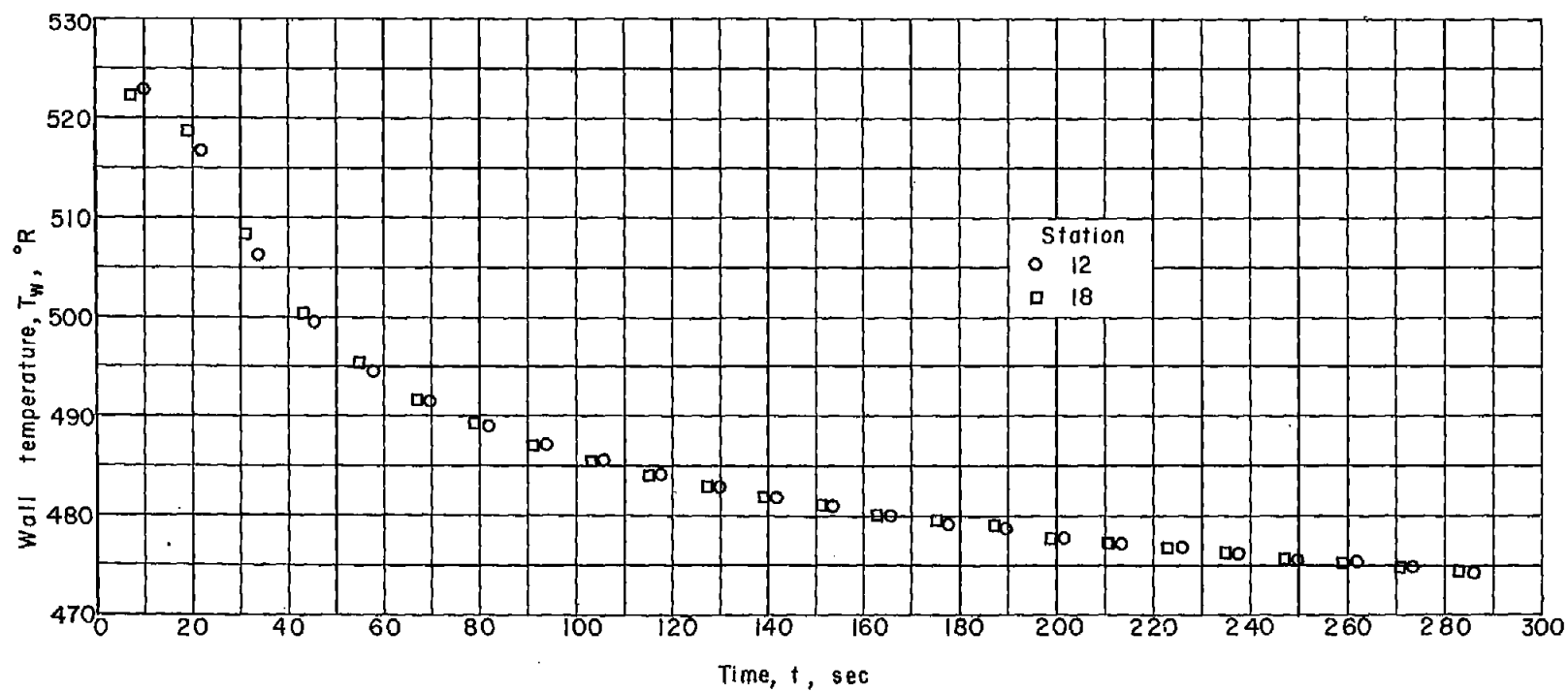


Figure 4.- Variation of wall temperature with time for settling-chamber pressure of 196 lb/sq in. gage.

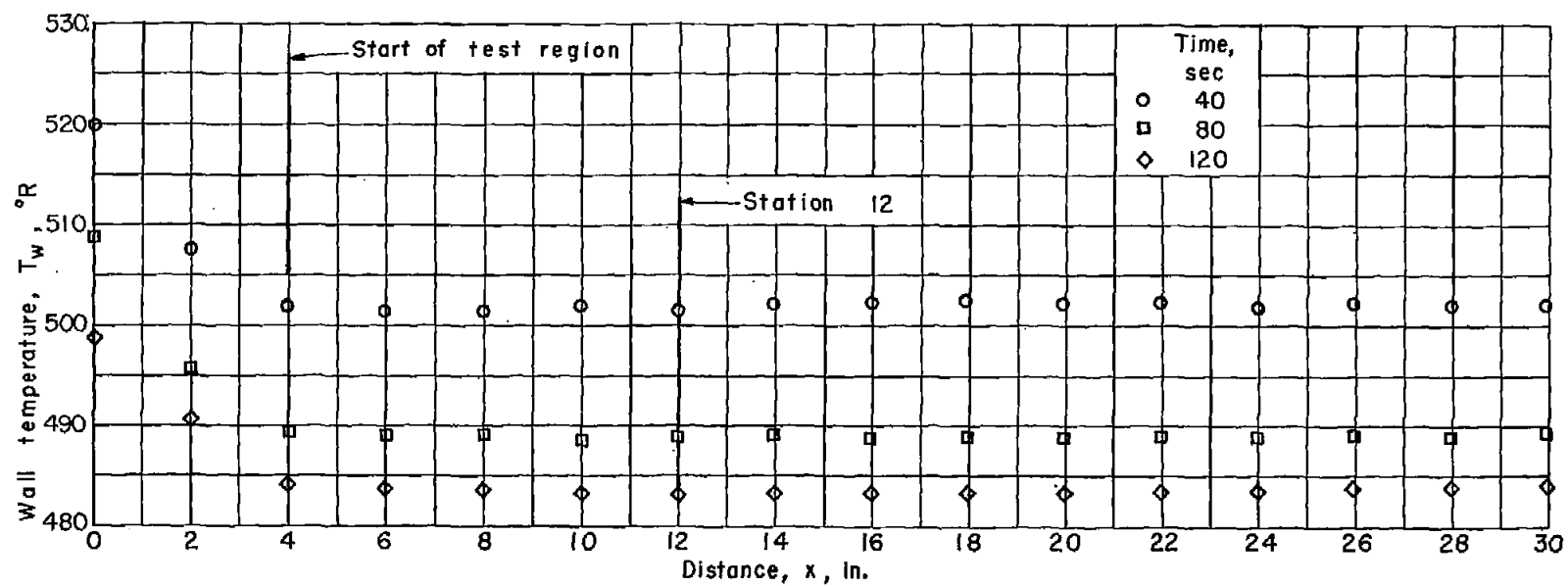


Figure 5.- Variation of wall temperature with longitudinal distance for settling-chamber pressure of 196 lb/sq in. gage.

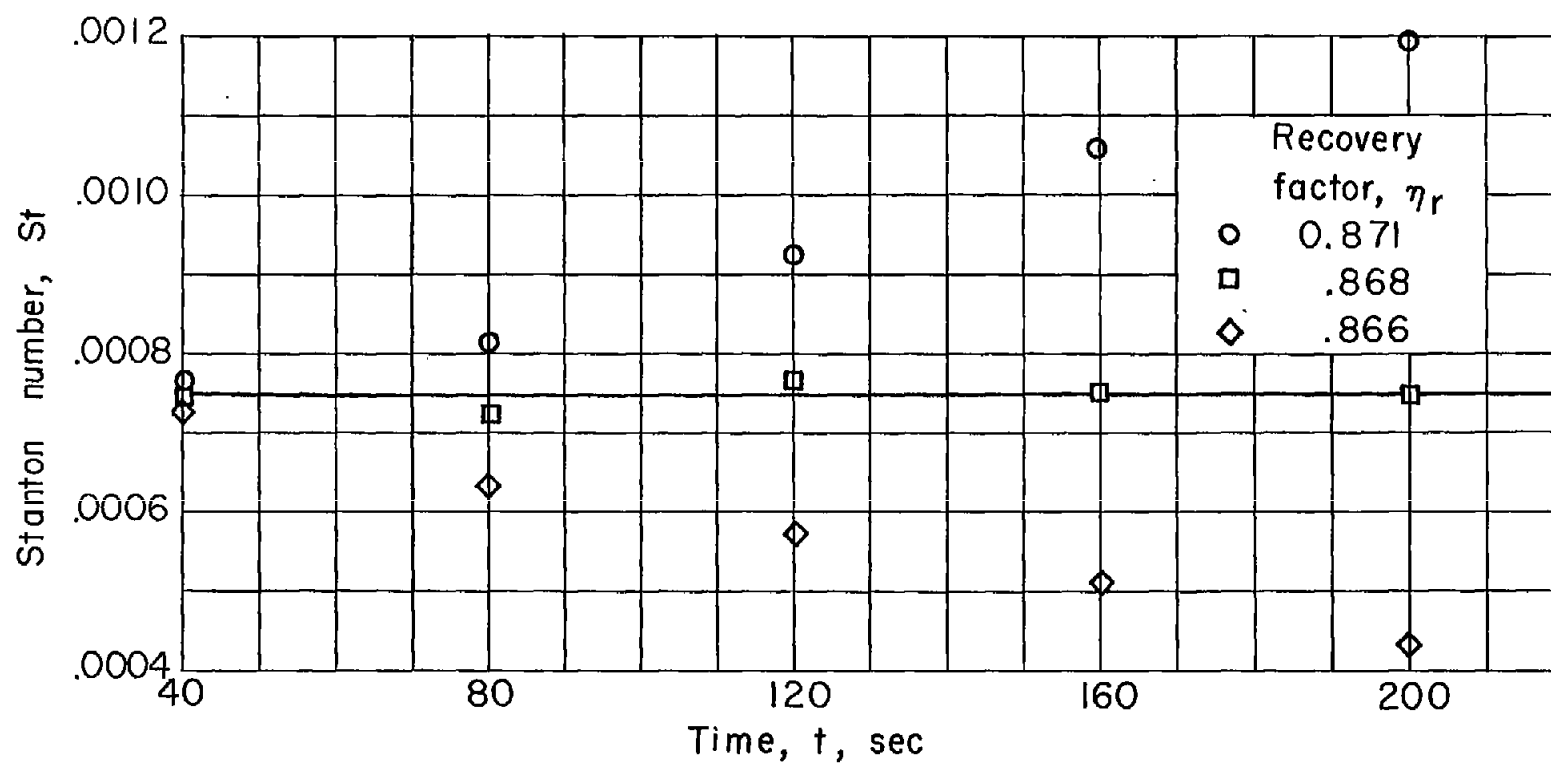


Figure 6.- Stanton number as a function of time and recovery factor at station 12 for settling-chamber pressure of 196 lb/sq in. gage.

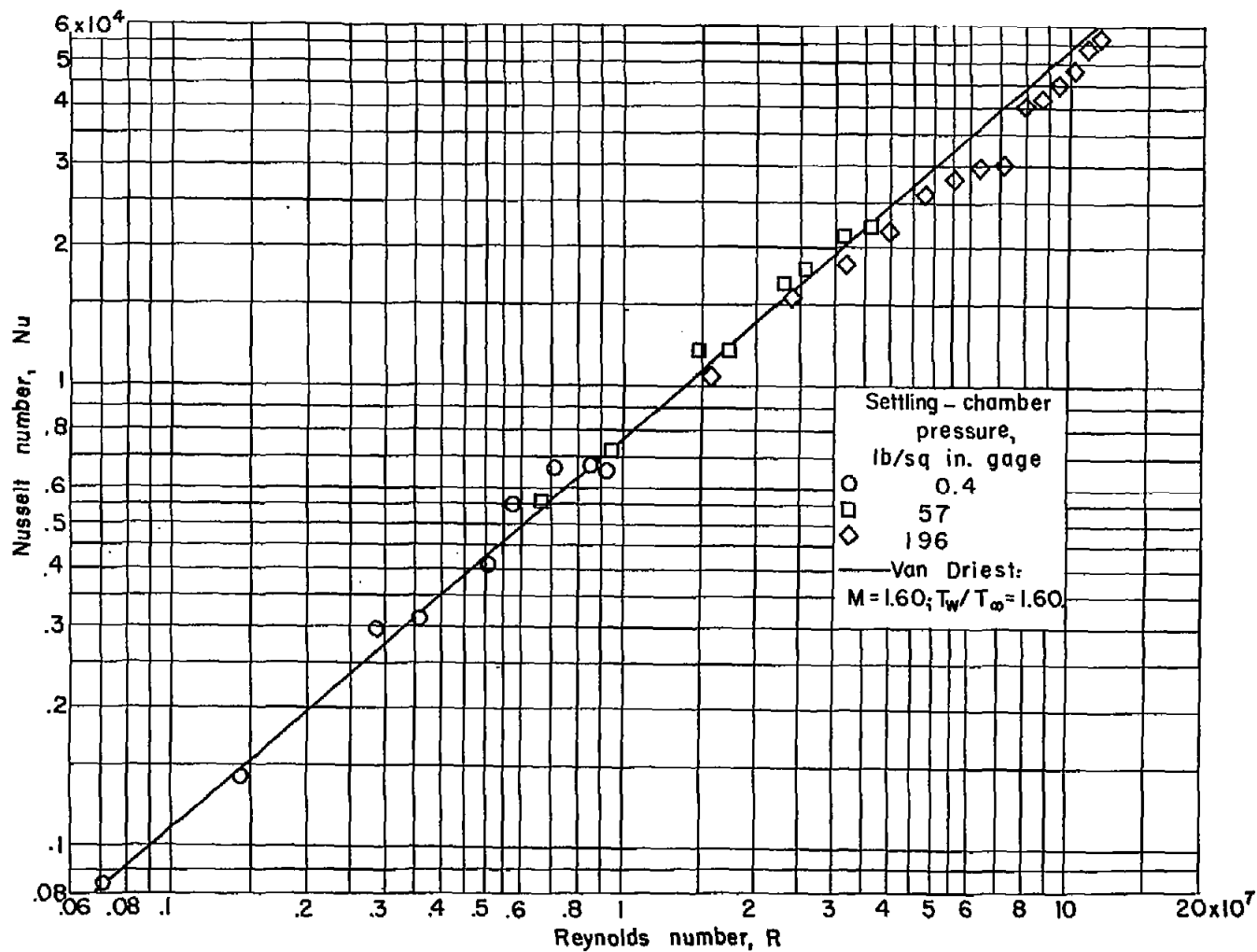


Figure 7.- Variation of local Nusselt number with local Reynolds number for adjusted locations of  $x = 0$ . Viscosity and Prandtl number determined for wall temperatures.

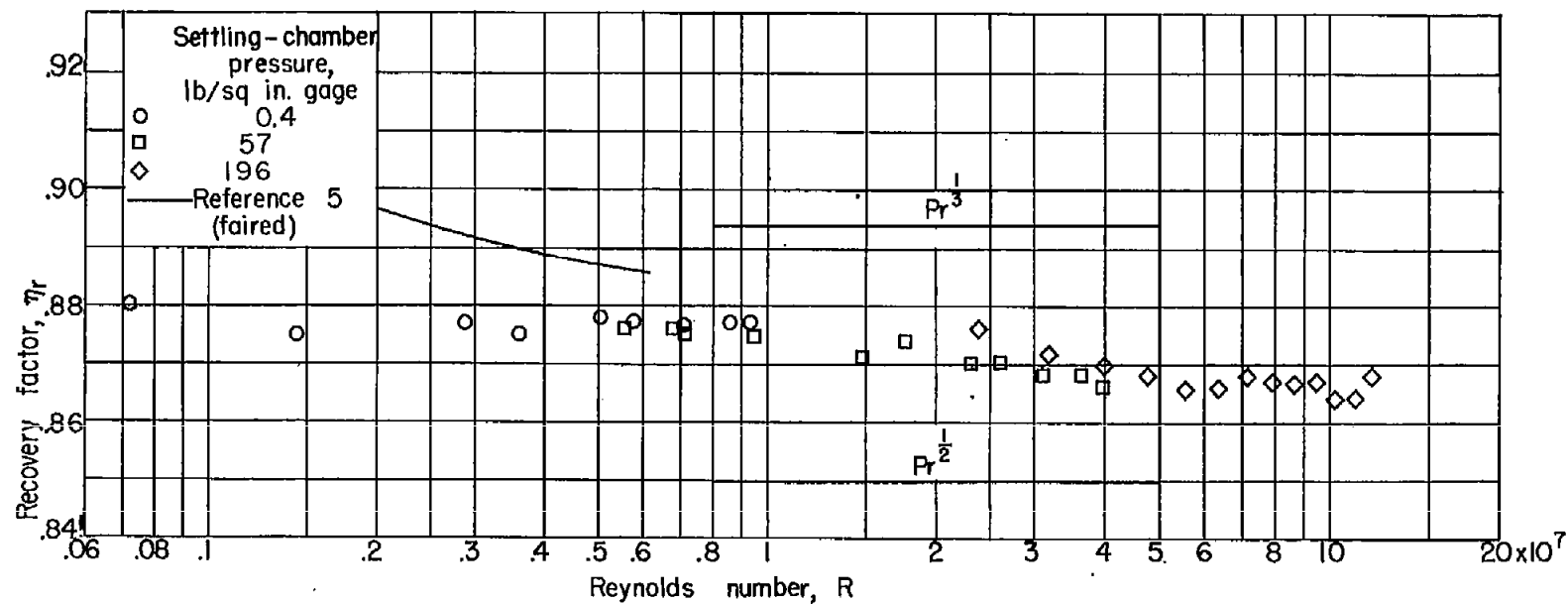


Figure 8.- Variation of local recovery factor with local Reynolds number for adjusted locations of  $x = 0$ . Viscosity determined for wall temperatures.